

Electronic Supplementary Information (ESI) for Chemical Communications

This journal is (c) The Royal Society of Chemistry 2021

# Nanowired $\text{NiMoO}_4/\text{NiSe}_2/\text{MoSe}_2$ prepared through in situ selenylation as high performance supercapacitor electrode

Chengchao Wang, Datong Wu, Yong Qin and Yong Kong\*

Jiangsu Key Laboratory of Advanced Materials and Technology, School of Petrochemical Engineering, Changzhou University, Changzhou 213164, China

Email address: yzkongyong@cczu.edu.cn

## Experimental section

**Reagents and apparatus.** Nickel nitrate hexahydrate ( $\text{Ni}(\text{NO}_3)_2 \cdot 6\text{H}_2\text{O}$ ), sodium molybdate dihydrate ( $\text{Na}_2\text{MoO}_4 \cdot 2\text{H}_2\text{O}$ ), potassium hydroxide (KOH) and anhydrous alcohol were purchased from Sinopharm Chemical Reagent Co., Ltd. (Shanghai, China). Selenium (Se) powder was obtained from Aladdin Chemistry Co., Ltd. (Shanghai, China). All aqueous solutions were prepared with ultrapure water ( $18.2 \text{ M}\Omega \cdot \text{cm}$ , Millipore).

In situ selenylation of  $\text{NiMoO}_4$  was conducted in a model OTL1200 quartz tube furnace purchased from Nanjing Nanda Instrument Plant (Nanjing, China). The morphologies of different samples were characterized with a Supra55 field-emission scanning electron microscope (FESEM, Zeiss, Germany) and a JEM 2100 transmission electron microscope (TEM, JEOL, Japan), respectively. The X-ray diffraction (XRD) patterns were recorded on a D/max 2500PC diffractometer (Rigaku, Japan). Nitrogen adsorption-desorption isotherms and the pore size distributions of different samples were determined by using an ASAP 2010 specific surface area and pore size analyzer (Micromeritics, USA). Chemical analysis of  $\text{NiMoO}_4$  and  $\text{NiMoO}_4/\text{NiSe}_2/\text{MoSe}_2$  was conducted by X-ray photoelectron spectroscopy (XPS) (ESCALAB 250Xi, Thermo Fisher Scientific, USA). All electrochemical measurements including cyclic voltammetry, galvanostatic charge-discharge (GCD) testing and electrochemical impedance spectroscopy (EIS) were carried out on a CHI660D electrochemical workstation (CH Instruments, Inc., China). The electrical conductivities of different samples were measured by using a model SZT-2A four-probe instrument obtained from Tongchuang Electronics Co., Ltd. (Suzhou, China).

**Synthesis of  $\text{NiMoO}_4$  nanowire.**  $\text{NiMoO}_4$  nanowire was synthesized by a simple hydrothermal method previously reported.<sup>1</sup> In a typical procedure, 436.2 mg (1.5 mmol) of  $\text{Ni}(\text{NO}_3)_2 \cdot 6\text{H}_2\text{O}$  and 362.9 mg (1.5 mmol) of  $\text{Na}_2\text{MoO}_4 \cdot 2\text{H}_2\text{O}$  were dissolved in the mixture of 25 mL anhydrous alcohol and 25 mL water with magnetic stirring for 30 min. Next, the mixture was transferred into a Teflon-lined stainless-steel autoclave of 100 mL and maintained at 160 °C for 4 h. The products were thoroughly rinsed with water and anhydrous alcohol several times, and then dried at 60 °C in an oven for 12 h. Finally, the  $\text{NiMoO}_4$  nanowire was obtained by annealing at 500 °C in an argon atmosphere for 2 h.

**Synthesis of nanowired NiMoO<sub>4</sub>/NiSe<sub>2</sub>/MoSe<sub>2</sub>.** The nanowired NiMoO<sub>4</sub>/NiSe<sub>2</sub>/MoSe<sub>2</sub> ternary nanocomposite was synthesized through in situ selenylation of NiMoO<sub>4</sub> with Se powder. The Se powder of different masses (0.1, 0.2, and 0.3 g) and 0.1 g NiMoO<sub>4</sub> were placed into two porcelain boats, respectively, which were then transferred into the quartz tube furnace and calcined at 400 °C in an argon atmosphere for 2 h. The obtained products were denoted as NiMoO<sub>4</sub>/NiSe<sub>2</sub>/MoSe<sub>2</sub>-x (x = 1, 2, and 3).

**Electrochemical measurements.** All the electrochemical experiments were conducted in a traditional three-electrode cell consisting of a NiMoO<sub>4</sub> or NiMoO<sub>4</sub>/NiSe<sub>2</sub>/MoSe<sub>2</sub>-x modified glassy carbon electrode (GCE, 3 mm in diameter) as the working electrode, a platinum foil as the auxiliary electrode and a KCl saturated calomel electrode (SCE) as the reference electrode. The electrolyte used in these electrochemical experiments was 2.0 M KOH aqueous solution. The working electrode was fabricated by dropping 10 µL of the dispersion of NiMoO<sub>4</sub> or NiMoO<sub>4</sub>/NiSe<sub>2</sub>/MoSe<sub>2</sub>-x (2 mg mL<sup>-1</sup>) onto the GCE surface and allowed to dry in ambient air.

Cyclic voltammograms (CVs) were recorded over the potential range between 0 and 0.5 V, and the GCD curves were collected over the potential range between -0.1 and 0.45 V. The cyclic stability of NiMoO<sub>4</sub> and NiMoO<sub>4</sub>/NiSe<sub>2</sub>/MoSe<sub>2</sub>-x was assessed by repeating the GCD testing for 5,000 cycles at the current density of 10 A g<sup>-1</sup>. EIS was conducted in the frequency range from 10<sup>5</sup> to 0.01 Hz with an alternating sinusoidal signal of 5 mV at the open circuit potential of 0.1 V, and the equivalent circuit was simulated by the ZSimpWin software.

**Calculation of specific capacitances.** The specific capacitances of different active samples can be calculated from both the CVs and the GCD curves.<sup>2</sup> For the CVs, the specific capacitance is calculated by the following equation:  $C_s = \frac{\int IdV}{mvV}$ , where  $C_s$  represents the specific capacitance (F g<sup>-1</sup>),  $I$  is the current (A),  $m$  is the mass of the active materials (g),  $v$  is the scan rate (V s<sup>-1</sup>) and  $V$  is the potential (V). For the GCD curves, the specific capacitance is obtained by the following equation:  $C_s = \frac{I \times t}{m \times V}$ , where  $C_s$  is the specific capacitance (F g<sup>-1</sup>),  $I$  represents the current (A),  $t$  represents the discharge time (s),  $m$  represents the mass of the active materials (g), and  $V$  represents the potential change during the discharge process (V).

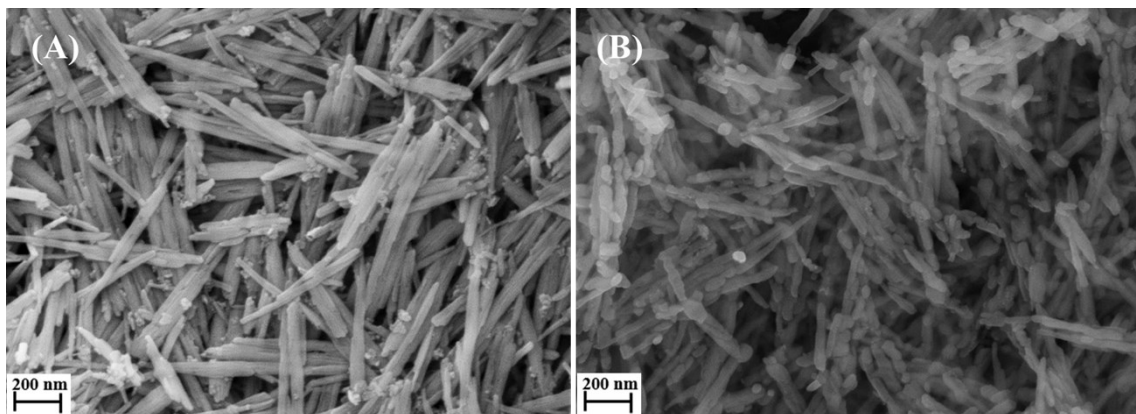


**Figure S1** SEM images before (A) and after (B) the selenylation of  $\text{NiMoO}_4$ .

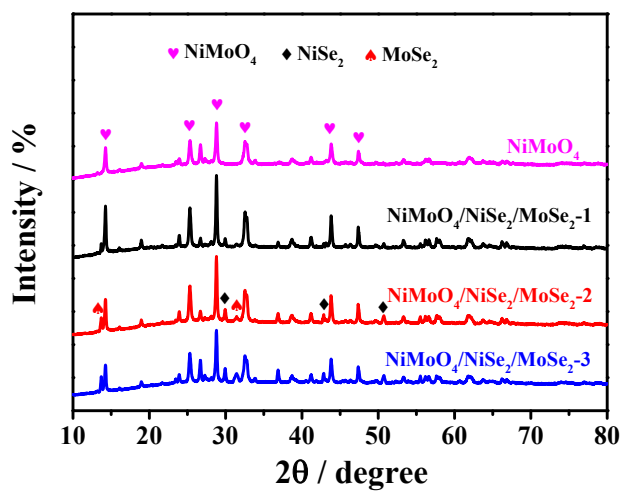


**Figure S2** XRD patterns of  $\text{NiMoO}_4$  and  $\text{NiMoO}_4/\text{NiSe}_2/\text{MoSe}_2$ -x (x = 1, 2, and 3).

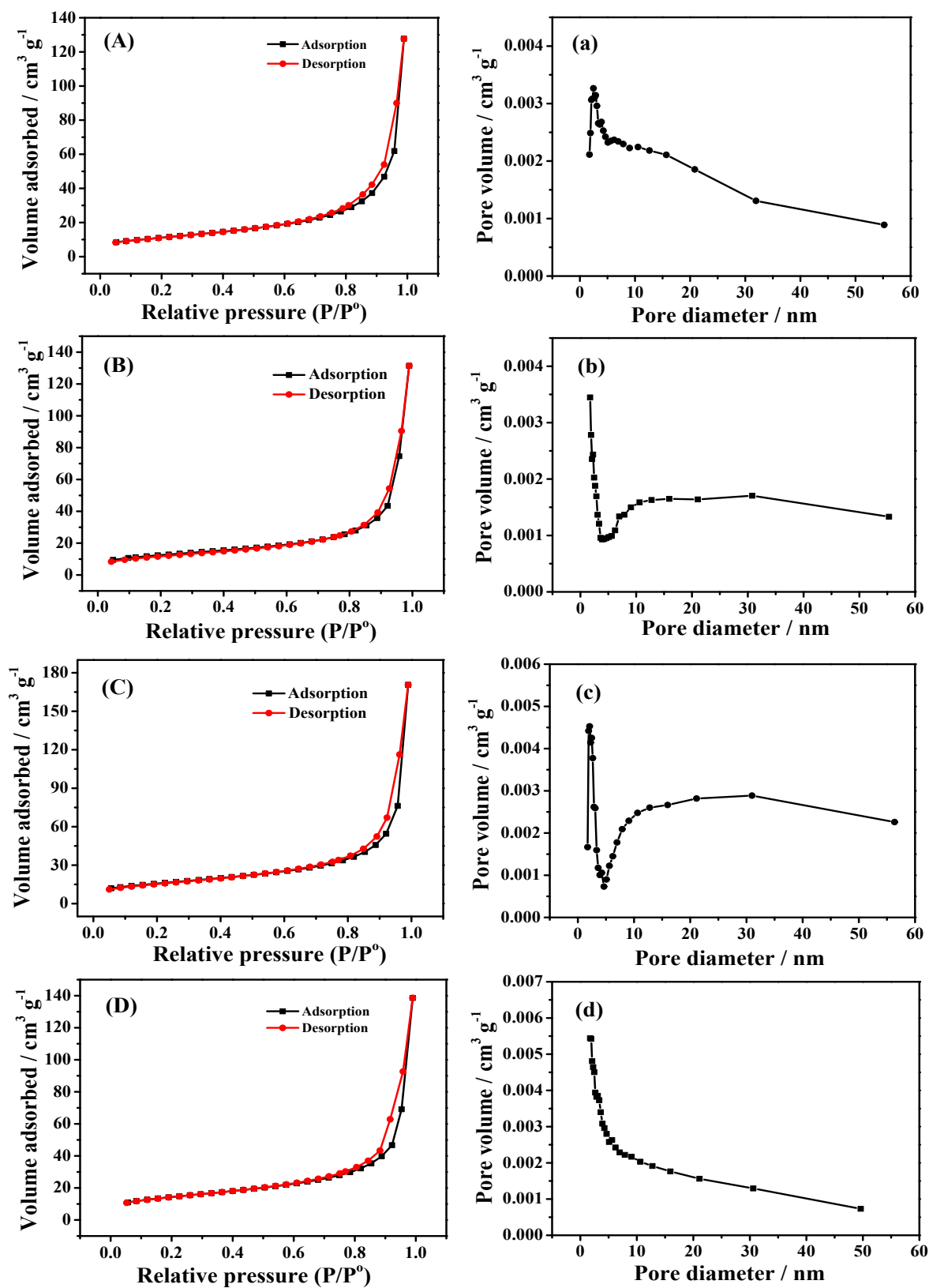


**Figure S3** N<sub>2</sub> adsorption-desorption isotherms of NiMoO<sub>4</sub> (A) and NiMoO<sub>4</sub>/NiSe<sub>2</sub>/MoSe<sub>2</sub>-x (x = 1, 2, and 3) (B–D) at 77 K. Pore size distribution of NiMoO<sub>4</sub> (a) and NiMoO<sub>4</sub>/NiSe<sub>2</sub>/MoSe<sub>2</sub>-x (x = 1, 2, and 3) (b–d).

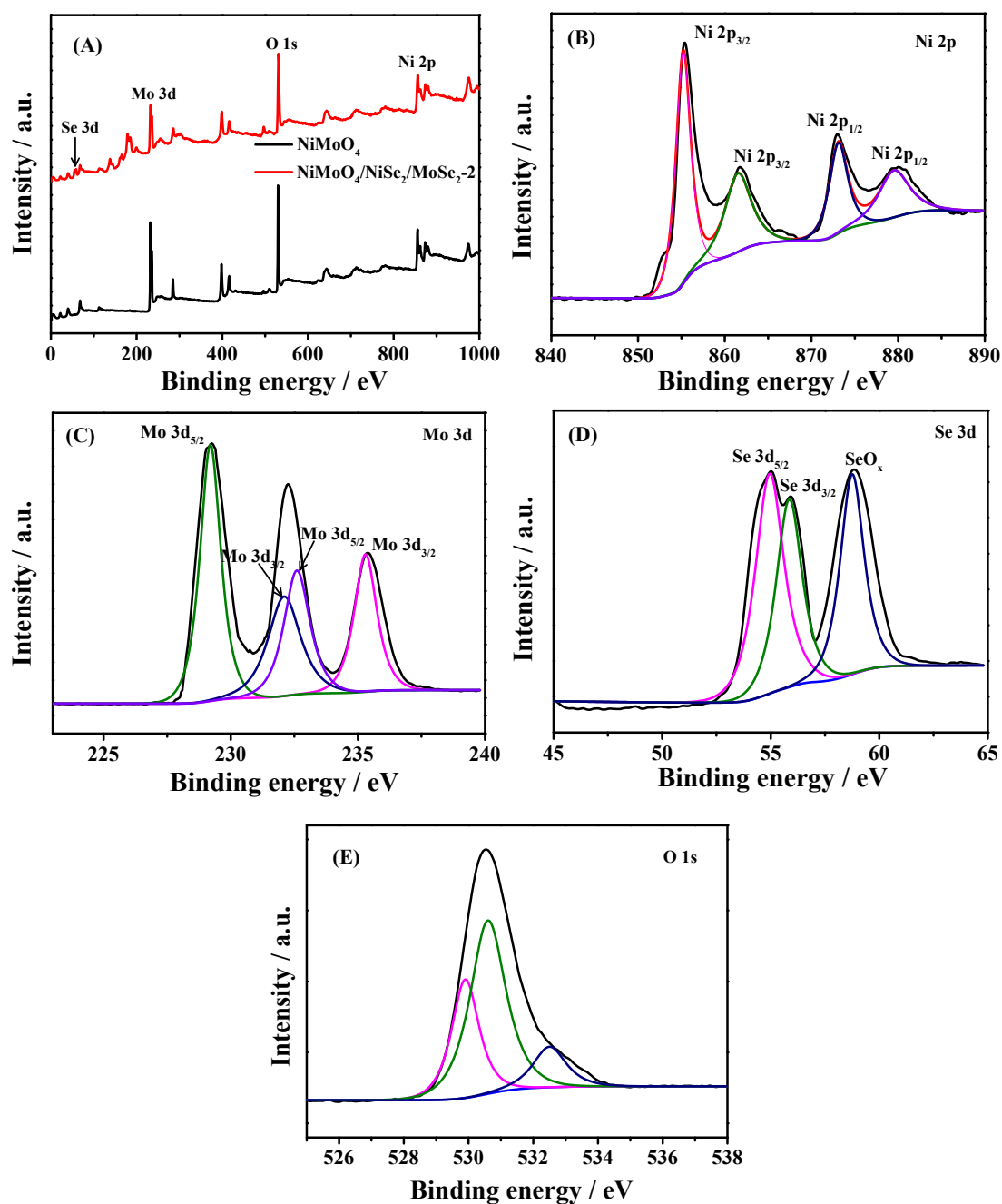


**Figure S4** (A) Survey XPS spectra of  $\text{NiMoO}_4$  and  $\text{NiMoO}_4/\text{NiSe}_2/\text{MoSe}_2\text{-2}$ , and high-resolution Ni 2p (B), Mo 3d (C), Se 3d (D) and O 1s (E) XPS spectra of  $\text{NiMoO}_4/\text{NiSe}_2/\text{MoSe}_2\text{-2}$ .

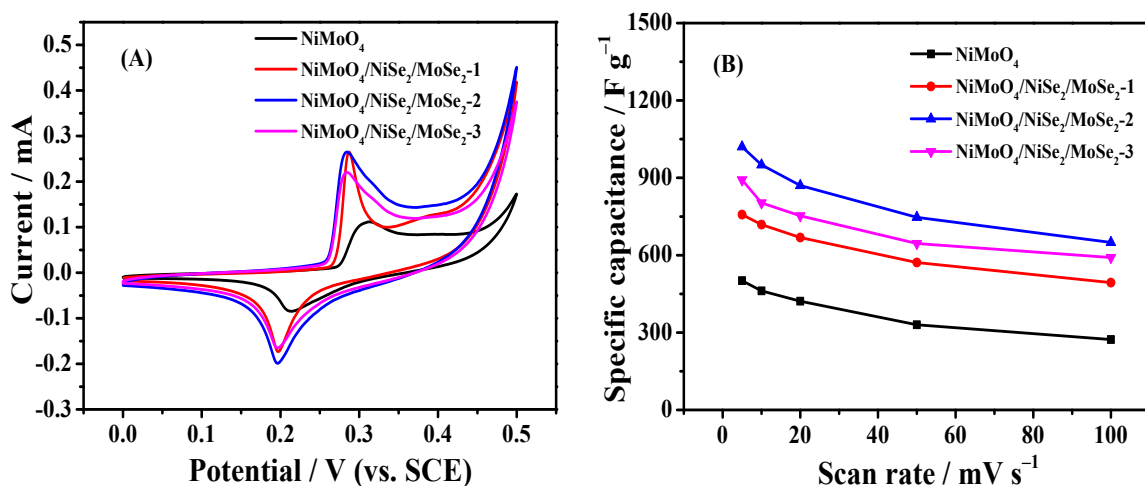


**Figure S5** (A) Cyclic voltammograms of GCE modified with NiMoO<sub>4</sub> and NiMoO<sub>4</sub>/NiSe<sub>2</sub>/MoSe<sub>2</sub>-x (x = 1, 2, and 3) in 2.0 M KOH at the scan rate of 5 mV s<sup>-1</sup>. (B) Specific capacitances of NiMoO<sub>4</sub> and NiMoO<sub>4</sub>/NiSe<sub>2</sub>/MoSe<sub>2</sub>-x (x = 1, 2, and 3) in 2.0 M KOH at different scan rates.

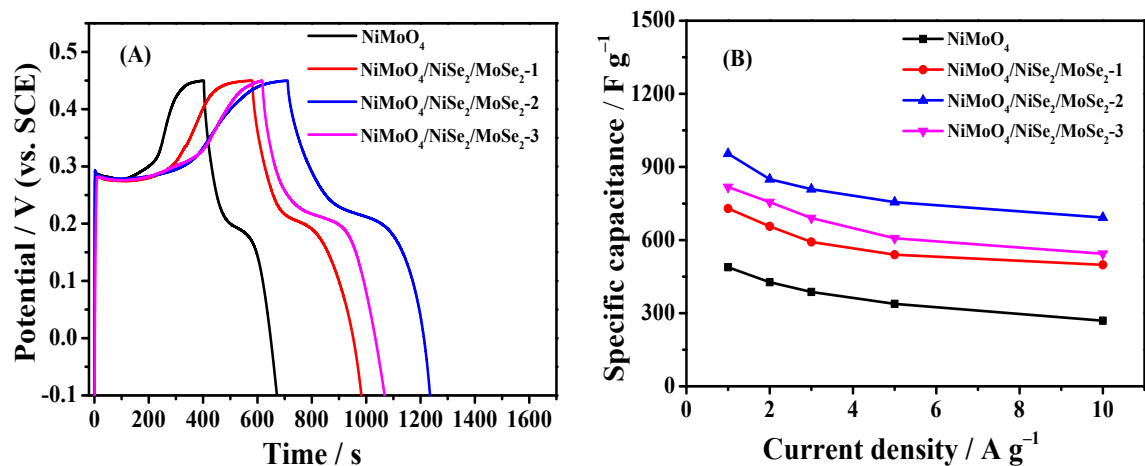


**Figure S6** (A) GCD curves of GCE modified with NiMoO<sub>4</sub> and NiMoO<sub>4</sub>/NiSe<sub>2</sub>/MoSe<sub>2</sub>-x (x = 1, 2, and 3) in 2.0 M KOH at the current density of 1 A g<sup>-1</sup>. (B) Specific capacitances of NiMoO<sub>4</sub> and NiMoO<sub>4</sub>/NiSe<sub>2</sub>/MoSe<sub>2</sub>-x (x = 1, 2, and 3) in 2.0 M KOH at different current densities.

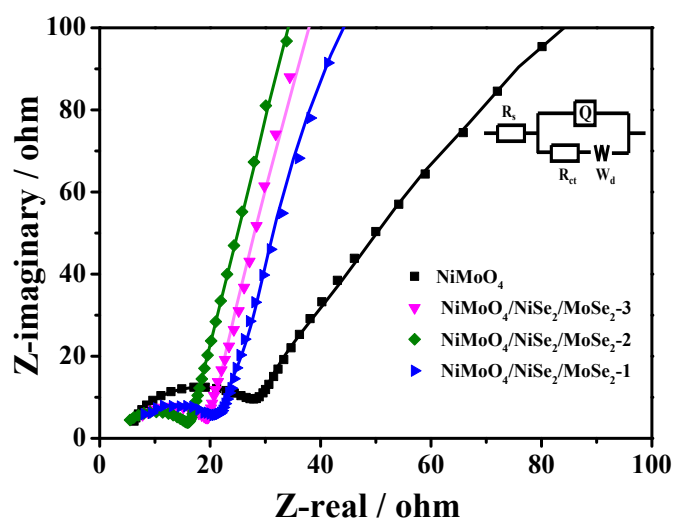


**Figure S7** Nyquist plots of  $\text{NiMoO}_4$  and  $\text{NiMoO}_4/\text{NiSe}_2/\text{MoSe}_2\text{-}x$  ( $x = 1, 2$ , and  $3$ ) in  $2.0 \text{ M KOH}$ . Inset is the corresponding equivalent circuit, where  $R_s$  represents the ohmic resistance of electrolyte and the internal resistance of electrode,  $R_{ct}$  represents the interfacial charge transfer resistance,  $W_d$  represents the Warburg resistance, and  $Q$  represents the constant phase element.

**Table S1** Performance comparison with the previously reported results at the current density of  $1 \text{ A g}^{-1}$ .

Sample	Capacitance	Electrolyte	Reference
$\text{MnO}_2@\text{NiMoO}_4$	$582.2 \text{ F g}^{-1}$	$2 \text{ M KOH}$	3
$\text{NiMoO}_4/\text{MnMoO}_4$	$430 \text{ F g}^{-1}$	$3 \text{ M KOH}$	4
$\text{NiMoO}_4/\text{ZnMoO}_4$	$556 \text{ F g}^{-1}$	$3 \text{ M KOH}$	4
$\text{NiMoO}_4/\text{CoMoO}_4$	$740 \text{ F g}^{-1}$	$3 \text{ M KOH}$	4
$\text{NiMoO}_4/\text{NiSe}_2/\text{MoSe}_2$	$955 \text{ F g}^{-1}$	$2 \text{ M KOH}$	This work

**Table S2** Electrical conductivities of different active materials.

Active material	Electrical conductivity (S cm <sup>-1</sup> )
NiMoO <sub>4</sub>	2.1
NiMoO <sub>4</sub> /NiSe <sub>2</sub> /MoSe <sub>2</sub> -1	340.1
NiMoO <sub>4</sub> /NiSe <sub>2</sub> /MoSe <sub>2</sub> -2	806.5
NiMoO <sub>4</sub> /NiSe <sub>2</sub> /MoSe <sub>2</sub> -3	487.8

## References

- 1 C. Qing, C. X. Yang, M. Y. Chen, W. H. Li, S. Y. Wang and Y. W. Tang, *Chem. Eng. J.*, 2018, **354**, 182.
- 2 B. H. Wang, Y. Qin, W. S. Tan, Y. X. Tao and Y. Kong, *Electrochim. Acta*, 2017, **241**, 1.
- 3 X. H. Wang, H. Y. Xia, J. Gao, B. Shi, Y. Fang, M. W. Shao, *J. Mater. Chem. A*, 2016, **10**, 1039.
- 4 Y. Zhang, C. R. Chang, X. D. Jia, Y. Cao, J. Yan, H. W. Luo, H. L. Gao, Y. Ru, H. X. Mei, A. Q. Zhang, K. Z. Gao, L. Z. Wang, *Inorg. Chem. Commun.*, 2020, **112**, 107697.